Chapter 14
Speed Control of Induction Motor Servo Drives Using Terminal Sliding-Mode Controller

Yong Feng, Minghao Zhou, Fengling Han and Xinghuo Yu

14.1 Introduction

The induction motor (IM) is one of the most common electrical motor used in most applications. This motor runs at a speed less than its synchronous speed, therefore it is also called as asynchronous motor. The synchronous speed is the speed of rotation of the magnetic field in a rotary machine and it depends upon the frequency and number poles of the IM. The IM has been extensively used in many practical applications due to its simply construction, lower repair and maintenance costs, high reliability and relatively low manufacturing cost, etc [1]. With the development of power electronics, electrical technique and control theories, IMs have been able to be used in high-performance servo systems, such as speed servo systems, even position servo systems.

Three methods can be used for the control of IMs: the scalar control, the direct torque control (DTC) and the field oriented control (FOC). The former method is very simple method for controlling the speed of IM compared to the vector control which is more complex. The latter two methods can be utilized to implement the high-performance IM servo systems.

Y. Feng (✉) · M. Zhou
Department of Electrical Engineering, Harbin Institute of Technology,
Harbin 150001, People's Republic of China
e-mail: yfeng@hit.edu.cn

M. Zhou
e-mail: zhouminghao@aliyun.com

F. Han
School of Science, RMIT University, Melbourne, VIC 3001, Australia
e-mail: fengling.han@rmit.edu.au

X. Yu
Research & Innovation Portfolio, RMIT University, Melbourne, VIC 3001, Australia
e-mail: x.yu@rmit.edu.au

S. Li et al. (eds.), *Advances in Variable Structure Systems and Sliding Mode Control—Theory and Applications*, Studies in Systems, Decision and Control 115, DOI 10.1007/978-3-319-62896-7_14

In DTC-based IM servo systems both the stator flux and the torque are regulated respectively using the bang-bang control strategies. This control method may lead to the torque ripple. If the IM runs at low speed, its performances will become poorer, and the speed range will be limited.

FOC is widely used in high performance control of IM servo systems. Since the torque and flux of an IM are decoupled using FOC, the IM systems can yield faster dynamic response and lower steady-state error. The mathematical model of an IM in a three-dimensional stationary reference frame (abc) can be converted into a model in a two-dimensional rotating reference frame (dq) using the Clarke-Park transformation. The d-axis current in the stator represents the rotor flux and the q-axis current represents the torque. Therefore, the decoupled rotor flux and the torque of an IM can be separately controlled like as a decoupled excited DC motor. Consequently it is possible to achieve good steady-state and dynamic performances of IMs [2, 3].

However, an accurate information on both the magnitude and the angular position of the rotor flux are needed by FOC for the transformation between the rotating and the stationary reference frames. There are two main methods for obtaining the magnitude and the angular position of the rotor flux, the direct measurements or the indirect estimation. The former needs special sensors, therefore it is difficult in practical applications. The latter is popular and widely used [4]. It applies the measurements of the stator currents, stator voltages and the motor speed into some estimation algorithms to estimate the magnitude and the angular position of the rotor flux. A lot of estimation methods for the rotor flux have been proposed, such as Luenberger observer-based methods [5, 6], model reference methods [7, 8], Kalman filter-based methods [9], and neural networks [10].

The high performance control of IMs is a challenge due to multi-variable, strong coupling, and nonlinearities in the model of IMs [11, 12]. So far, a lot of control methods have been proposed to improve the robustness and dynamical performances of IMs, such as neural network control, fuzzy control, optimal control, adaptive control and sliding-mode control [13, 14]. Sliding-mode control has attractive advantages compared to other control methods, such as low sensitivity to the system parameter variations and strong robustness to external disturbances [15, 16]. However, the chattering phenomena limit the practical applications of conventional sliding-mode control [17]. In this chapter, a nonsingular terminal sliding-mode control (NTSM) method is applied for IM velocity servo systems. To implement the FOC of IMs, an NTSM observer is designed in the chapter to estimate the rotor flux of IMs with equivalent smooth control signals [18, 19]. Additionally, the speed sensorless technology is also utilized in this chapter, afterwards an NTSM observer is utilized in the FOC system of IMs to estimate the speed instead of practical sensors.The simulations have been carried out to validate the applied method.

14.2 Mathematical Model of Induction Motor

An accurate mathematical model of IMs is the basic factor for the implementation of high-performance servo systems of IMs, especially for the FOC algorithms. For simplicity of the analysis some assumptions for IMs can be described as follows:

(1) the effect of magnetic saturation is neglected.

(2) the three-phase windings have the same structure and the fringe effect is neglected.

(3) the slots effect is ignored.

(4) the iron core loss is not taken into account.

14.2.1 Mathematical Model of IM in Three-Dimensional Stationary Coordinate (abc)

The mathematical model of IMs is usually composed of the voltage, flux, and motion equations. Based on the assumptions above, the voltage equations of the IMs in three-dimensional stationary coordinate (abc) are below:

$$\begin{bmatrix} u_{sa} \\ u_{sb} \\ u_{sc} \\ u_{ra} \\ u_{rb} \\ u_{rc} \end{bmatrix} = \begin{bmatrix} R_s & 0 & 0 & 0 & 0 & 0 \\ 0 & R_s & 0 & 0 & 0 & 0 \\ 0 & 0 & R_s & 0 & 0 & 0 \\ 0 & 0 & 0 & R_r & 0 & 0 \\ 0 & 0 & 0 & 0 & R_r & 0 \\ 0 & 0 & 0 & 0 & 0 & R_r \end{bmatrix} \begin{bmatrix} i_{sa} \\ i_{sb} \\ i_{sc} \\ i_{ra} \\ i_{rb} \\ i_{rc} \end{bmatrix} + \begin{bmatrix} \dot{\psi}_{sa} \\ \dot{\psi}_{sb} \\ \dot{\psi}_{sc} \\ \dot{\psi}_{ra} \\ \dot{\psi}_{rb} \\ \dot{\psi}_{rc} \end{bmatrix} \tag{14.1}$$

where u_{sa}, u_{sb} and u_{sc} are three stator voltages in abc axes;
u_{ra}, u_{rb} and u_{rc} are three rotor voltages in abc axes;
i_{sa}, i_{sb} and i_{sc} are three stator currents in abc axes;
i_{ra}, i_{rb} and i_{rc} are three rotor currents in abc axes;
ψ_{sa}, ψ_{sb} and ψ_{sc} are three stator fluxes in abc axes;
ψ_{ra}, ψ_{rb} and ψ_{rc} are three rotor fluxes in abc axes;
R_s is the stator resistance;
R_r is the rotor resistance.

Therefore the flux equations of an IM in the three-dimensional stationary coordinate (abc) include both the stator and rotor flux equations and describe the relationships between the currents and the fluxes in the stator and rotor. They are given by the following equations:

$$\begin{bmatrix} \psi_s \\ \psi_r \end{bmatrix} = \begin{bmatrix} L_{ss} & L_{sr} \\ L_{rs} & L_{rr} \end{bmatrix} \begin{bmatrix} i_s \\ i_r \end{bmatrix} \tag{14.2}$$

with

$$L_{ss} = \begin{bmatrix} L_{sm}+L_{sl} & -\frac{1}{2}L_{sm} & -\frac{1}{2}L_{sm} \\ -\frac{1}{2}L_{sm} & L_{sm}+L_{sl} & -\frac{1}{2}L_{sm} \\ -\frac{1}{2}L_{sm} & -\frac{1}{2}L_{sm} & L_{sm}+L_{sl} \end{bmatrix}, L_{rr} = \begin{bmatrix} L_{sm}+L_{rl} & -\frac{1}{2}L_{sm} & -\frac{1}{2}L_{sm} \\ -\frac{1}{2}L_{sm} & L_{sm}+L_{rl} & -\frac{1}{2}L_{sm} \\ -\frac{1}{2}L_{sm} & -\frac{1}{2}L_{sm} & L_{sm}+L_{rl} \end{bmatrix},$$

$$L_{sr} = L_{rs}^{T} = L_{sm} \begin{bmatrix} \cos\theta & \cos(\theta-120°) & \cos(\theta+120°) \\ \cos(\theta+120°) & \cos\theta & \cos(\theta-120°) \\ \cos(\theta-120°) & \cos(\theta+120°) & \cos\theta \end{bmatrix}$$

where ψ_s and ψ_r are the stator flux phase and the rotor flux phase in abc axes respectively, by $\psi_s = [\psi_{sa}, \psi_{sb}, \psi_{sc}]^T$, $\psi_r = [\psi_{ra}, \psi_{rb}, \psi_{rc}]^T$

$\boldsymbol{i}_s$ and $\boldsymbol{i}_r$ are the stator current vector and the rotor current vector in abc axes respectively, by $\boldsymbol{i}_s = [\boldsymbol{i}_{sa}, \boldsymbol{i}_{sb}, \boldsymbol{i}_{sc}]^T$, $\boldsymbol{i}_r = [\boldsymbol{i}_{ra}, \boldsymbol{i}_{rb}, \boldsymbol{i}_{rc}]^T$;

L_{sl} and L_{rl} are the stator and rotor leakage inductance respectively;

L_{sm} and L_{rm} are the mutual inductance between the stator and rotor windings;

θ is the electric angle between the stator and rotor windings.

The torque equation of IMs can be given as follows:

$$\begin{aligned} T_e = n_p L_{sm}[&(i_{sa}i_{ra} + i_{sb}i_{rb} + i_{sc}i_{rc})\sin\theta + (i_{sa}i_{ra} + i_{sb}i_{rb} + i_{sc}i_{rc})\sin(\theta+120°) \\ &+ (i_{sa}i_{ra} + i_{sb}i_{rb} + i_{sc}i_{rc})\sin(\theta-120°)] \end{aligned} \tag{14.3}$$

where n_p is the number of pole pairs.

Finally the mechanical equation of an IM can be described as follows:

$$T_e = T_L + \frac{J}{n_p}\dot{\omega} \tag{14.4}$$

where ω is the electric angular velocity of the rotor;

J is the inertia of the motor;

T_L is the load torque.

14.2.2 Mathematical Model of IM in Two-Dimensional Stationary Coordinate ($\alpha\beta$)

Based on Clarke transformation, the mathematical model of IMs in a three-dimensional stationary coordinate (abc) can be converted into a two-dimensional stationary coordinate ($\alpha\beta$). The Clarke transformation is given by the following equation:

$$\boldsymbol{C}_{3/2} = \sqrt{\frac{2}{3}} \begin{bmatrix} 1 & -\frac{1}{2} & -\frac{1}{2} \\ 0 & \frac{\sqrt{3}}{2} & \frac{\sqrt{3}}{2} \end{bmatrix} \tag{14.5}$$

Subsequently, the voltage equations of the IMs in a two-dimensional stationary coordinate ($\alpha\beta$) can be described as follow:

$$\begin{cases} u_{s\alpha} = R_s i_{s\alpha} + L_s \dot{i}_{s\alpha} + L_m \dot{i}_{r\alpha} \\ u_{s\beta} = R_s i_{s\beta} + L_s \dot{i}_{s\beta} + L_m \dot{i}_{rb} \\ u_{r\alpha} = R_r i_{r\alpha} + L_r \dot{i}_{r\alpha} + L_m \dot{i}_{r\alpha} + \omega(L_m i_{s\beta} + L_r i_{r\beta}) \\ u_{r\beta} = R_r i_{r\beta} + L_r \dot{i}_{r\beta} + L_m \dot{i}_{s\beta} + \omega(\mathrm{L}_m i_{s\alpha} + L_r i_{r\alpha}) \end{cases} \tag{14.6}$$

where $u_{s\alpha}$ and $u_{s\beta}$ are two stator voltages in $\alpha\beta$ axes;
$u_{r\alpha}$ and $u_{r\beta}$ are two rotor voltages in $\alpha\beta$ axes;
$i_{s\alpha}$ and $i_{s\beta}$ are two stator currents in $\alpha\beta$ axes;
$i_{r\alpha}$ and $i_{r\beta}$ are two rotor currents in $\alpha\beta$ axes;
L_s, L_r, and L_m the stator inductance, the rotor inductance and the mutual inductance between the stator and rotor windings, which are described by

$$L_s = L_m + L_{ls},\ L_r = L_m + L_{lr},\ L_m = \frac{3}{2} L_{ms}$$

Then the flux equations of IMs in a two-dimensional stationary coordinate ($\alpha\beta$) can be described as follow:

$$\begin{cases} \psi_{s\alpha} = L_s i_{s\alpha} + L_m i_{r\alpha} \\ \psi_{s\beta} = L_s i_{s\beta} + L_m i_{r\beta} \\ \psi_{r\alpha} = L_m i_{s\alpha} + L_r i_{r\alpha} \\ \psi_{r\beta} = L_m i_{s\beta} + L_r i_{r\beta} \end{cases} \tag{14.7}$$

where $\psi_{s\alpha}$ and $\psi_{s\beta}$ are the stator fluxes in $\alpha\beta$ axes respectively;
$\psi_{r\alpha}$ and $\psi_{r\beta}$ are the rotor fluxes in axes respectively.
The torque equation of IMs in a two-dimensional stationary coordinate ($\alpha\beta$) is described as follows:

$$T_e = n_p L_m (i_{s\beta} i_{r\alpha} - i_{s\alpha} i_{r\beta}) \tag{14.8}$$

14.2.3 Mathematical Model of IMs in Two-Dimensional Rotating Coordinate (dq)

The FOC strategy can decouple the d-axis and q-axis currents in the stator of an IM applying the Park transformation, and make the rotor flux and torque of the IM controlled separately like as decoupled excited DC motors. The relationship between the two-dimensional stationary and rotating coordinates can be shown in Fig. 14.1, where θ_e represents the electric angle between the d-axis and the α-axis. The speed of the two-dimensional rotating coordinate equals to ω_1 which is the synchronous electric angular velocity of the IM.

The Park transformation is given by

$$\boldsymbol{C}_{2s/2r} = \begin{bmatrix} \cos\theta_e & \sin\theta_e \\ -\sin\theta_e & \cos\theta_e \end{bmatrix} \tag{14.9}$$

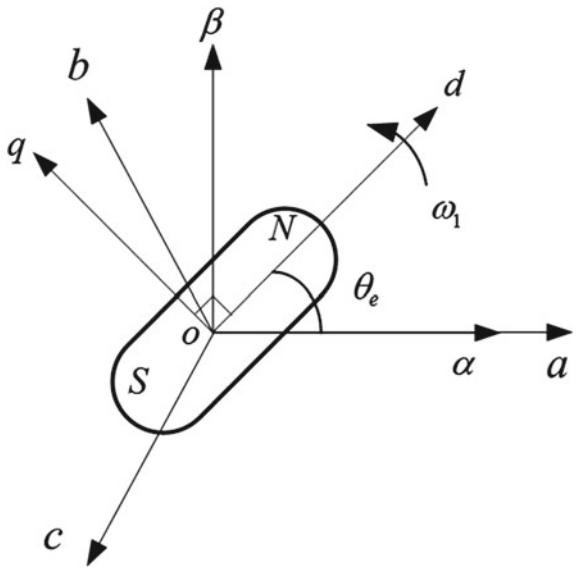

Fig. 14.1 $\alpha\beta$ and dq coordinates

Then the voltage equations of the IMs in a two-dimensional rotating coordinate (dq) can be described as follow:

$$\begin{cases} u_{sd} = R_s i_{sd} + \dot{\psi}_{sd} - \omega_1 \psi_{sq} \\ u_{sq} = R_s i_{sq} + \dot{\psi}_{sq} + \omega_1 \psi_{sd} \\ u_{rd} = R_r i_{rd} + \dot{\psi}_{rd} - \omega_s \psi_{rq} \\ u_{rq} = R_r i_{rq} + \dot{\psi}_{rq} - \omega_s \psi_{rd} \end{cases} \tag{14.10}$$

where u_{sd} and u_{sq} are two stator voltages in dq axes;
u_{rd} and u_{rq} are two rotor voltages in dq axes;
i_{sd} and i_{sq} are the stator currents in d- and q- axes;
i_{rd} and i_{rq} are the rotor currents in d- and q- axes;
ψ_{sd} and ψ_{sq} are the stator fluxes in d- and q- axes;
ψ_{rd} and ψ_{rq} are the rotor fluxes in d- and q- axes;
ω_s is the slip angle velocity;
ω_1 is the synchronous angular velocity.

The flux equations of the IMs in a two-dimensional rotating coordinate system (dq) can be described as follow:

$$\begin{cases} \psi_{sd} = L_s i_{sd} + L_m i_{rd} \\ \psi_{sq} = L_s i_{sq} + L_m i_{rq} \\ \psi_{rd} = L_m i_{sd} + L_r i_{rq} \\ \psi_{rq} = L_m i_{sq} + L_r i_{rq} \end{cases} \tag{14.11}$$

The torque equation of IMs in a two-dimensional rotating coordinate (dq) is given by

$$T_e = \frac{n_p L_m}{L_r}(i_{sq}\psi_{rd} - i_{sd}\psi_{rq}) \tag{14.12}$$

Summarizing, the mathematical model of IMs in a three-dimensional stationary coordinate (abc) is described by Eqs.(14.1)–(14.4), which is further transferred to the model in a two-dimensional stationary coordinate $(\alpha\beta)$, as shown as in Eqs. (14.6), (14.7) and (14.8), by the Clark transformation (14.5). Finally, the model of IMs in a two-dimensional rotating coordinate (dq) is obtained in Eqs. (14.4), (14.10), (14.11) and (14.12) by the Park transformation (14.9).

14.3 Field Oriented Control System

For squirrel cage IMs, the rotor voltages are

$$u_{rd} = u_{rq} = 0 \tag{14.13}$$

The mathematical model of the IMs in the FOC systems can be finally described in dq axes as follows by using Eqs. (14.4), and (14.10)–(14.13):

$$\begin{cases} \dot{i}_{sd} = \xi\frac{1}{T_r}\psi_{rd} + \xi\omega\psi_{rq} - \lambda i_{sd} + \omega_1 i_{sq} + K u_{sd} \\ \dot{i}_{sq} = -\xi\omega\psi_{rd} + \xi\frac{1}{T_r}\psi_{rq} - \omega_1 i_{sd} - \lambda i_{sq} + K u_{sq} \\ \dot{\psi}_{rd} = -\frac{1}{T_r}\psi_{rd} + (\omega_1 - \omega)\psi_{rq} + \frac{L_m}{T_r} i_{sd} \\ \dot{\psi}_{rq} = -(\omega_1 - \omega)\psi_{rd} - \frac{1}{T_r}\psi_{rq} + \frac{L_m}{T_r} i_{sq} \\ \dot{\omega} = \frac{n_p^2 L_m}{J L_r}\left(i_{sq}\psi_{rd} - i_{sd}\psi_{rq}\right) - \frac{n_p}{J} T_L \end{cases} \tag{14.14}$$

where $\sigma = 1 - L_m^2/L_s L_r$ is the leakage coefficient; $T_r = L_r/R_r$ is the rotor time constant; and $K = 1/\sigma L_s$, $\xi = K(L_m/L_r)$, $\lambda = K(R_s + L_m^2/T_r L_r)$.

Based on the FOC strategy, the d-axis is orientated in accord with the axis of the rotor flux. Therefore d- and q- axis rotor flux can be determined as follows

$$\begin{cases} \psi_{rd} = \psi_r \\ \psi_{rq} = 0 \end{cases} \tag{14.15}$$

where ψ_r is the rotor flux.

The FOC of IMs is based on their mathematical model (14.14) and the field orientated principle (14.15). It can be seen that the control of IMs is decoupled into the rotor flux control and torque control. Then the FOC-based speed servo system of IMs can be built using four nonsingular terminal sliding-mode controllers in

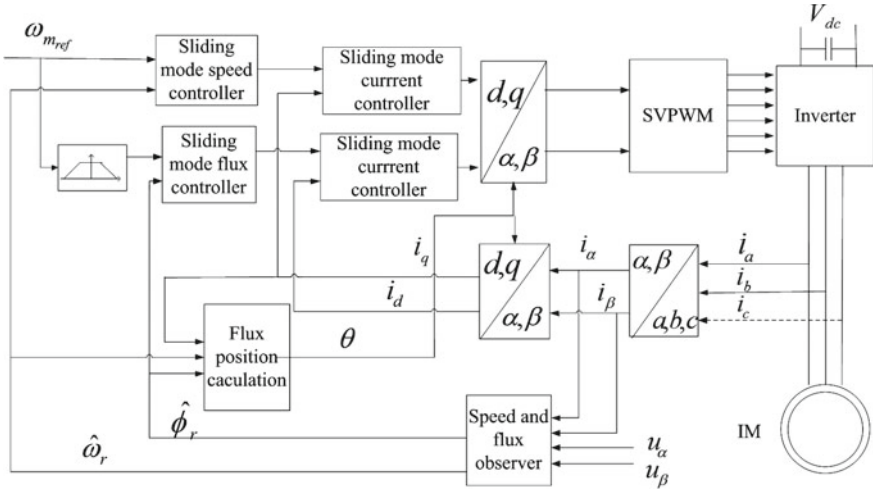

Fig. 14.2 An FOC-based speed closed-loop control system of IMs

the speed-, flux-, d-axis current- and q-axis current-loops respectively, as shown in Fig. 14.2.

In Fig. 14.2, $\omega_{m_{ref}}$ is the required speed of the IM. The outputs of the speed and flux controllers are the references of the stator currents in d- and q-axes respectively. To implement high-performance control of the FOC position servo system of IMs, four full-order sliding-mode controllers will be designed in the next section.

14.4 NTSM Controllers for IM Servo System

14.4.1 Speed Controller

The motion equation of the IMs can be obtained from the model of the IMs (14.14) as follows:

$$\dot{\omega}_m = \frac{n_p L_m}{J L_r} i_{sq} \psi_r - \frac{1}{J} T_L \tag{14.16}$$

where $\omega_m = \omega / n_p$ is the mechanical angular velocity of the rotor.

Defining the desired mechanical velocity of the motor as $\omega_{m_{ref}}$, which should be smooth enough up to the second order time derivative, the error between the actual velocity and the given velocity e_ω is:

$$e_\omega = \omega_{m_{ref}} - \omega_m \tag{14.17}$$

Then the speed error dynamics can be obtained as follows using Eqs.(14.16) and (14.17):

$$\dot{e}_\omega = \dot{\omega}_{m_{ref}} - \dot{\omega}_m = \dot{\omega}_{m_{ref}} - \frac{n_p L_m}{J L_r}\psi_r i_{sq} + \frac{1}{J}T_L \tag{14.18}$$

A NTSM manifold [7] is designed as follows:

$$s_\omega = e_\omega + \gamma_1 \dot{e}_\omega^{p_1/q_1} \tag{14.19}$$

where $\gamma_1 > 0$; p_1 and q_1 are odd, and $1 < p_1/q_1 < 2$.

Theorem 14.1 *The NTSM surface (14.19) and the following control assure that finite-time convergence of the speed error dynamics (14.18):*

$$i_{sq_{ref}} = i_{sq_{eq}} + i_{sq_n} \tag{14.20}$$

$$i_{sq_{eq}} = \frac{J L_r}{n_p L_m \psi_r}\dot{\omega}_{m_{ref}} \tag{14.21}$$

$$\dot{i}_{sq_n} + T i_{sq_n} = v_\omega \tag{14.22}$$

$$v_\omega = \frac{J L_r}{n_p L_m \psi_r}\left(\frac{s_\omega \dot{e}_\omega^{p_1/q_1-1}}{\left|s_\omega \dot{e}_\omega^{p_1/q_1-1}\right|^2}|s_\omega|\left|\dot{e}_\omega^{p_1/q_1-1}\right|(k_1+\eta_1) + \frac{q_1}{\gamma_1 p_1}\dot{e}_\omega^{2-p_1/q_1}\right) \tag{14.23}$$

where $k_1 > 0$, $\eta_1 > 0$ are design parameters, and $k_1 > \left(\left|\frac{1}{J}\dot{T}_L\right| + \left|\frac{n_p L_m \psi_r}{J L_r} T i_{sq_n}\right|\right)$.

Proof The following Lyapunov function is considered $V_\omega(t) = 0.5{s_\omega}^2(t)$. We have:

$$\dot{V}_\omega(t) = s_\omega(t)\dot{s}_\omega(t) = s_\omega\left[\dot{e}_\omega + \frac{\gamma_1 p_1}{q_1}\dot{e}_\omega^{p_1/q_1-1}\ddot{e}_\omega\right]$$

$$= \frac{s_\omega \gamma_1 p_1}{q_1}\dot{e}_\omega^{p_1/q_1-1}\left[-\frac{n_p L_m}{J L_r}\psi_r \dot{i}_{sq_n} + \frac{1}{J}\dot{T}_L + \frac{q_1}{\gamma_1 p_1}\dot{e}_\omega^{2-p_1/q_1}\right]$$

$$= \frac{s_\omega \gamma_1 p_1}{q_1}\dot{e}_\omega^{p_1/q_1-1}\left[-\frac{n_p L_m \psi_r}{J L_r}v_\omega + \frac{n_p L_m \psi_r}{J L_r}T i_{sq_n} + \frac{1}{J}\dot{T}_L + \frac{q_1}{\gamma_1 p_1}\dot{e}_\omega^{2-p_1/q_1}\right]$$

$$= \frac{s_\omega \gamma_1 p_1}{q_1} \dot{e}_\omega^{p_1/q_1-1} \left[-\frac{s_\omega \dot{e}_\omega^{p_1/q_1-1}}{\left| s_\omega \dot{e}_\omega^{p_1/q_1-1} \right|^2} |s_\omega| \left| \dot{e}_\omega^{p_1/q_1-1} \right| (k_1 + \eta_1) + \frac{n_p L_m \psi_r}{J L_r} T i_{sq_n} + \frac{1}{J} \dot{T}_L \right]$$

$$= \frac{\gamma_1 p_1}{q_1} \left[-|s_\omega| \left| \dot{e}_\omega^{p_1/q_1-1} \right| (k_1 + \eta_1) + s_\omega \dot{e}_\omega^{p_1/q_1-1} \left(\frac{1}{J} \dot{T}_L + \frac{n_p L_m \psi_r}{J L_r} T i_{sq_{ref}} \right) \right]$$

$$\leq \frac{\gamma_1 p_1}{q_1} |s_\omega| \left| \dot{e}_\omega^{p_1/q_1-1} \right| \left[-(k_1 + \eta_1) + \left| \frac{1}{J} \dot{T}_L \right| + \left| \frac{n_p L_m \psi_r}{J L_r} T i_{sq_{ref}} \right| \right]$$

$$\leq \frac{\gamma_1 p_1}{q_1} \eta_1 \left| \dot{e}_\omega^{p_1/q_1-1} \right| |s_\omega|$$

since $k_1 > \left(\left| \dot{T}_L / J \right| + \left| (n_p L_m \psi_r / J L_r) T i_{sq_{ref}} \right| \right)$, therefore

$$\dot{V}_\omega(t) \leq -\gamma_1 (p_1/q_1) \eta_1 \left| \dot{e}_\omega^{p_1/q_1-1} \right| |s_\omega| \, | < 0 \quad \text{for } |s_\omega| \neq 0$$

which means that the speed error dynamics (14.18) can reach the sliding-mode surface in finite time, and then both e_ω and $\dot{e}_\omega$ can converge to zero within infinite time. This completes the proof.

14.4.2 Rotor Flux Controller Design

Define the desired rotor flux as $\psi_{r_{ref}} = \text{sconst}$, the error between the actual rotor flux and the desired flux is e_ψ:

$$e_\psi = \psi_{r_{ref}} - \psi_r \tag{14.24}$$

The rotor flux error system can be obtained as follows according to the mathematical model (14.14):

$$\dot{e}_\psi = -\dot{\psi}_r = \frac{1}{T_r} \psi_r - \frac{L_m}{T_r} i_{sd} \tag{14.25}$$

The sliding-mode surface s_ψ is designed as the follows:

$$s_\psi = e_\psi + \gamma_2 \dot{e}_\psi^{p_2/q_2} \tag{14.26}$$

where $\gamma_2 > 0$, p_2, q_2 are odd, and $1 < p_2/q_2 < 2$.

Theorem 14.2 *The NTSM surface (14.26) and the following control assure the finite-time convergence of the rotor flux error system (14.25):*

$$i_{sd_{ref}} = i_{sd_{eq}} + i_{sd_n} \tag{14.27}$$

$$i_{sd_{eq}} = \frac{\psi_r}{L_m} \tag{14.28}$$

$$\dot{i}_{sd_n} + T i_{sd_n} = v_\psi \tag{14.29}$$

$$v_\psi = \frac{J L_r}{n_p L_m \psi_r} \left(\frac{s_\psi \dot{e}_\psi^{p_2/q_2 - 1}}{\left| s_\psi \dot{e}_\psi^{p_2/q_2 - 1} \right|^2} \left| s_\psi \right| \left| \dot{e}_\psi^{p_2/q_2 - 1} \right| (k_2 + \eta_2) + \frac{q_2}{\gamma_2 p_2} \dot{e}_\psi^{2 - p_2/q_2} \right) \tag{14.30}$$

where $k_2 > 0$, $\eta_2 > 0$ is the design parameter.

Proof This follows straightforwardly from Theorem 14.1.

14.4.3 q-axis Current Controller Design

Define the error between the desired current in q-axis ($i_{sq_{ref}}$) and the actual current in q-axis (i_{sq}) as follows:

$$e_{sq} = i_{sq_{ref}} - i_{sq} \tag{14.31}$$

The q-axis current error system can be obtained as the follow according to the mathematical model (14.14):

$$\dot{e}_{sq} = \dot{i}_{sq_{ref}} - \dot{i}_{sq} = \dot{i}_{sq_{ref}} + \xi \omega \psi_r + \omega_1 i_{sd} + \lambda i_{sq} - K u_{sq} \tag{14.32}$$

A NTSM manifold s_{sq} is designed as the follow:

$$s_{sq} = e_{sq} + \gamma_3 \dot{e}_{sq}^{p_3/q_3} \tag{14.33}$$

where $\gamma_3 > 0$, p_3, q_3 are odd, and $1 < p_3/q_3 < 2$.

Theorem 14.3 *The NTSM surface (14.33) and the following control assure the finite-time convergence of the q-axis current error system (14.32):*

$$u_{sq} = u_{sq_{eq}} + u_{sq_n} \tag{14.34}$$

$$u_{sq_{eq}} = \left(\dot{i}_{sq_{ref}} + \xi \omega \psi_r + \omega_1 i_{sd} + \lambda i_{sq} \right) / K \tag{14.35}$$

$$\dot{u}_{sq_n} + T u_{sq_n} = v_{sq} \tag{14.36}$$

$$v_{sq} = \frac{1}{K}\left(\frac{s_{sq}\dot{e}_{sq}^{p_3/q_3-1}}{\left|s_{sq}\dot{e}_{sq}^{p_3/q_3-1}\right|^2}\left|s_{sq}\right|\left|\dot{e}_{sq}^{p_3/q_3-1}\right|(k_3+\eta_3) + \frac{q_3}{\gamma_3 p_3}\dot{e}_{sq}^{2-p_3/q_3}\right) \tag{14.37}$$

where $k_3 > 0$, $\eta_3 > 0$ are design parameters.

Proof This follows straightforwardly from Theorem 14.1 as well.

14.4.4 d-axis Current Controller Design

Define the error between the desired and the actual d-axis current as the follow:

$$e_{sd} = i_{sd_{ref}} - i_{sd} \tag{14.38}$$

The d-axis current error system can be obtained as follows according to the mathematical model (14.14):

$$\dot{e}_{sd} = i_{sd_{ref}} - \xi\frac{1}{T_r}\psi_r + \lambda i_{sd} - \omega_1 i_{sq} - K u_{sd} \tag{14.39}$$

A NTSM manifold is designed as the follow:

$$s_{sd} = e_{sd} + \gamma_4 \dot{e}_{sd}^{p_4/q_4} \tag{14.40}$$

where $\gamma_4 > 0$, p_4 and q_4 are odd, and $1 < p_4/q_4 < 2$.

Theorem 14.4 *The NTSM surface (14.40) and the following control assure the finite-time convergence of the d-axis current error system (14.39):*

$$u_{sd} = u_{sd_{eq}} + u_{sd_n} \tag{14.41}$$

$$u_{sdeq} = \left(\dot{i}_{sd_{ref}} - \xi\frac{1}{T_r}\psi_r + \lambda i_{sd} - \omega_1 i_{sq}\right)/K \tag{14.42}$$

$$\dot{u}_{sd_n} + T u_{sd_n} = v_{sd} \tag{14.43}$$

$$v_{sd} = \frac{1}{K}\left(\frac{s_{sd}\dot{e}_{sd}^{p_4/q_4-1}}{\left|s_{sd}\dot{e}_{sd}^{p_4/q_4-1}\right|^2}\left|s_{sd}\right|\left|\dot{e}_{sd}^{p_4/q_4-1}\right|(k_4+\eta_4) + \frac{q_4}{\gamma_4 p_4}\dot{e}_{sd}^{2-p_4/q_4}\right) \tag{14.44}$$

where $k_4 > 0$, $\eta_4 > 0$ are parameters to design.

Proof This follows straightforwardly from Theorem 14.1.

14.5 Numerical Simulation Test

Some simulations are carried out for an IM control system to validate the applied NTSM controllers in MATLAB-Simulink. The parameters of the IM are give as follows:

$P_N = 1.1\,kW,\ I_N = 2.8\,A,\ U_N = 380\,V,\ f_N = 50\,Hz,\ n_p = 2,\ R_s = 5.9\,\Omega,\ R_r = 5.6\,\Omega,\ L_r = 37.94\,mH,\ L_s = 0.58\,H,\ L_m = 0.55\,H,\ J = 0.021\,kg \cdot m^2,\ \psi_{ref} = 0.7\,Wb.$

And the NTSM controllers are designed with the following parameters:

$p_1 = 5,\ q_1 = 3,\ \gamma_1 = 50,\ k_1 = 5000,\ T_1 = 10;\ p_2 = 5,\ q_2 = 3,\ \gamma_2 = 30,\ k_2 = 3000, T_2 = 10; p_3 = 7, q_3 = 5, \gamma_3 = 20, k_3 = 6000, T_3 = 5; p_4 = 13, q_4 = 11, \gamma_4 = 10,\ k_4 = 3000,\ T_4 = 5.$

The desired speed is $20sin(4t)$ rpm and the desired rotor flux is $0.7Wb$.

The motor speed and the its tracking error are displayed in Fig. 14.3. For clear observation, the desired speed is shifted a little bit manually. It can be seen that the motor speed can track its reference fast and accurately. The rotor flux and its tracking error are shown in Fig. 14.4. It is clear that the rotor flux can track its reference value reference. The desired flux is shifted a little as well. The stator currents are displayed in Fig. 14.5. Both of the two currents track their references quickly and accurately. The control signals of the NTSM current controllers are shown in Fig. 14.6. It can be seen that the two control signals are smooth, which means that the chattering is attenuated by the applied new high-order NTSM method, and better performances of IM systems can be obtained.

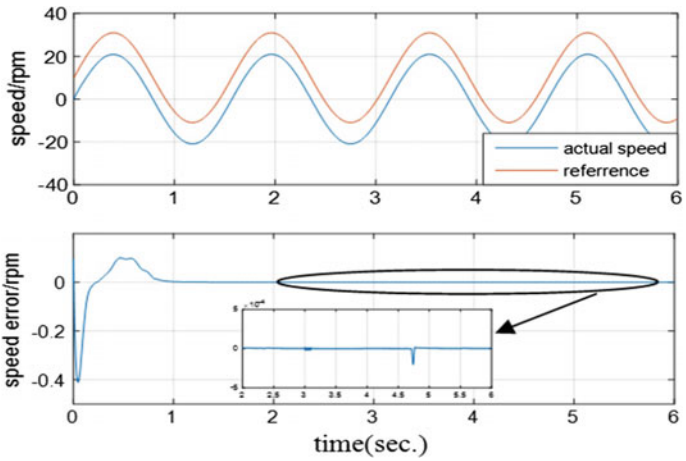

Fig. 14.3 The motor speed and its tracking error

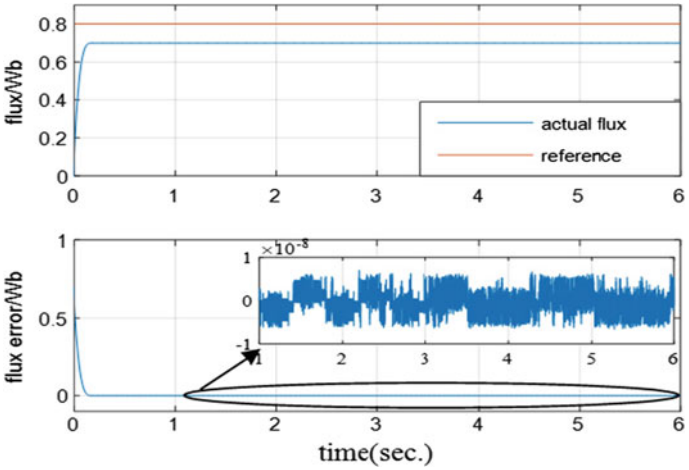

Fig. 14.4 The rotor flux and its tracking error

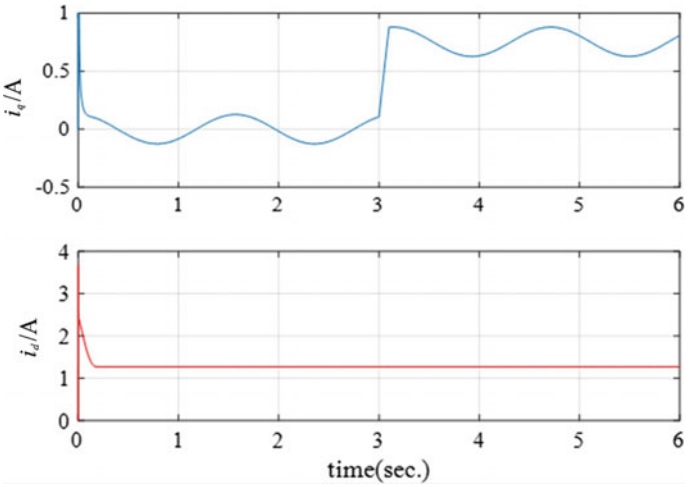

Fig. 14.5 The stator currents in dq

14.6 Conclusion

This chapter has introduced a nonsingular terminal sliding-mode control method for IM velocity servo systems. The NTSM controllers are applied into the speed, flux and current closed loop of the FOC-based IM velocity servo systems. The designed NTSM control law can suppress the chattering which exists in conventional sliding-mode control. The results of simulation have proved that the applied method is corrective and effective.

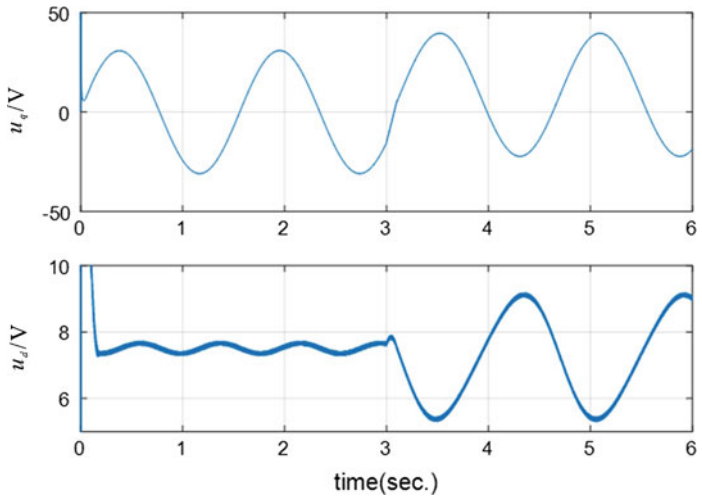

Fig. 14.6 The control signals of the NTSM current controllers

Acknowledgements This work was supported by the National Natural Science Foundation of China under Grant 61673132.

References

1. Zhou, M., Feng, Y., Yu, X.: High-order terminal sliding-mode observer for speed estimation of induction motors. In: Proceedings of the 8th IEEE Conference on Industrial Electronics and Applications, pp. 1045–1048 (2013)
2. Feng, Y., Zhou, M., Shi, H., Yu, X.: Flux estimation of induction motors using high-order terminal sliding-mode observer. In: Proceedings of 10th World Congress on Intelligent Control and Automation, pp. 1860–1863 (2012)
3. Feng, Y., Zheng, J., Yu, X., Truong, N.V.: Hybrid terminal sliding-mode observer design method for a permanent-magnet synchronous motor control system. IEEE Trans. Ind. Electron. **56**(9), 3424–3431 (2009)
4. Feng, Y., Zhou, M., Yu, X.: Sliding-Mode observer based flux estimation of induction motors. In: Proceedings of 5th International Conference on Intelligent Robotics and Applications, pp. 530–539 (2012)
5. Song, J., Lee, K.-B., Song, J.-H., Choy, I., Kim, K.-B.: Sensorless vector control of induction motor using a novel reduced-order extended Luenberger observer. In: Proceedings of Conference Record of the 2000 IEEE Industry Applications Conference, pp. 1828–1834 (2000)
6. Feng, Y., Yu, X., Han, F.: On nonsingular terminal sliding-mode control of nonlinear systems. Automatica **46**(6), 1715–1722 (2013)
7. Feng, Y., Yu, X., Man, Z.: Non-singular adaptive terminal sliding mode control of rigid manipulators. Automatica **38**(12), 2159–2167 (2002)
8. Camara, H.T., Carati, E.G., Hey, H.L., Pinheiro, H., Pinheiro, J.R., Grundling, H.A.: Speed and position servo for induction motor using robust model reference adaptive control. In: Proceedings of the 28th Annual Conference of the Industrial Electronics Society, pp. 1721–1727 (2002)

9. Feng, Y., Yu, X., Han, F.: High-order terminal sliding-mode observer for parameter estimation of a permanent-magnet synchronous motor. IEEE Trans. Ind. Electron. **60**(10), 4272–4280 (2013)
10. Lin, F.J., Wai, R.J.: Adaptive fuzzy-neural-network control for induction spindle motor drive. IEEE Trans. Energy Convers. **17**(4), 507–513 (2002)
11. Feng, Y., Yu, X., Zheng, X.: Second-order terminal sliding mode control of input-delay systems. Asian J. Control **8**(1), 12–20 (2006)
12. Feng, Y., Han, X., Wang, Y., Yu, X.: Second-order terminal sliding mode control of uncertain multivariable systems. Int. J. Control **80**(6), 856–862 (2007)
13. Feng, Y., Bao, S., Yu, X.: Design method of non-singular terminal sliding mode control systems. Control Decis. **17**(2), 194–198 (2002)
14. Zhou, M., Feng, Y.: High-order terminal sliding-mode control of uncertain systems with mismatched disturbance. In: Proceedings of 32nd Chinese Control Conference, pp. 3190–3193 (2013)
15. Zheng, J., Feng, Y., Lu, Q.: High-order terminal sliding-mode control for permanent magnet synchronous motor. Contr. Theory Appl. **26**(6), 697–700 (2009)
16. Wang, Y., Feng, Y., Lu, Q.: Design of free-chattering sliding mode control systems for permanent magnet synchronous motor. Electr. Mach. Control **2**(5), 514–519 (2008)
17. Feng, Y., Bao, S., Yu, X.: Inverse dynamics nonsingular terminal sliding mode control of two-link flexible manipulators. Int. J. Robot. Autom. **19**(2), 91–102 (2004)
18. Feng, Y., Yu, X., Man, Z.: Non-singular terminal sliding mode control and its application for robot manipulators. In: Proceedings of IEEE International Symposium on Circuits and Systems, pp. 545–548 (2001)
19. Zheng, X., Feng, Y., Bao, S.: Terminal sliding mode decomposed control of multivariable linear uncertain systems. Contr. Theory Appl. **21**(1), 11–16 (2004)